physica status solidi

pss

www.interscience.wiley.com

reprints

www.pss-rapid.com

www.pss-c.com

www.pss-b.com

www.pss-a.com

WILEY-VCH

REPRINT

Phys. Status Solidi B **247**, No. 9, 2218–2221 (2010) / **DOI** 10.1002/pssb.201046157

physica status solidi b
www.pss-b.com
basic solid state physics

Recombination activity of iron–boron pairs in compensated p-type silicon

Daniel Macdonald* **and An Liu**

School of Engineering, The Australian National University, Canberra ACT 0200, Australia

Received 16 February 2010, revised 1 April 2010, accepted 16 April 2010
Published online 17 May 2010

Keywords impurity levels, photoconductivity, p-type silicon, recombination

* Corresponding author: e-mail daniel.macdonald@anu.edu.au, Phone: +61 2 6125 2973, Fax: +61 2 6125 0506

Recently, the possible presence of boron–phosphorus pairs in compensated Si has been proposed in order to explain the unexpected behaviour of boron–oxygen defects in this material. These B–P pairs should also lead to an altered recombination activity of Fe-acceptor pairs in compensated Si, since some of the Fe-acceptor pairs would also be bound to P atoms, altering their energy level and carrier capture properties. In this work, we have used carrier lifetime measurements on Fe-implanted compensated Si wafers, containing both B and P, to identify the Fe-acceptor complexes present. The results indicate that FeB pairs dominate these samples, implying that Fe–B–P complexes, and by extension, B–P pairs, are unlikely to be present in significant concentrations.

1 Introduction Low-cost solar-grade silicon materials for solar cells are often strongly compensated, meaning they contain significant concentrations of both acceptors N_A and donors N_D. The impact of compensation on the relevant electronic properties for solar cells, such as carrier mobilities, lifetimes and defect formation, are topics of continuing research [1–4]. In particular, recent studies [2, 4] have shown that the concentration of the well-known boron–oxygen defect [5] in compensated Czochralski silicon (Cz-Si) does not scale with the boron concentration N_A, as initially expected, but instead with the net doping $p_0 = N_A - N_D$. The possible presence of B–P pairs, which could form during ingot cooling, and which might prohibit the formation of the boron–oxygen defect, has been proposed as one explanation for this observation [2, 4, 6].

However, such B–P pairs would also have other effects, providing opportunities to test for their presence. It has been shown previously that *all* of the B in compensated Si is available to bond with interstitial Fe at room temperature. This was demonstrated via measurement of the Fe-acceptor pairing rate, which scales with the *total* acceptor concentration in compensated silicon, rather than the net doping [7]. This means that if significant amounts of B–P pairs are present in compensated silicon, some form of Fe–B–P complexes would necessarily occur. Irrespective of the chemical likelihood of formation of such Fe–B–P complexes, they would be likely to have a different energy level and different capture cross sections to FeB pairs, which would lead to an altered impact on the carrier lifetime. In this work, we study the recombination activity of Fe-acceptor pairs in compensated p-type Si, into which a known dose of Fe has been introduced by ion implantation. This allows us to determine if the Fe is wholly present as FeB pairs, or if some other complex, such as Fe–B–P, is present. This in turn sheds light on the presence or otherwise of B–P pairs in compensated Si.

2 Experimental details The samples used were cleaved sections of $155 \times 155\,mm^2$ p-type, ⟨100⟩-oriented Cz-Si wafers from three B-doped control ingots (non-compensated), and two compensated ingots, doped with both B and P, as described elsewhere [4, 7]. Sections of the wafers were etched, cleaned and implanted with 70 keV Fe^{56} ions to a dose of $5 \times 10^{10}\,cm^{-2}$ on one surface. A $30 \times 30\,mm^2$ Si aperture was used to define the implantations. After further surface cleaning, the 140 μm thick samples were annealed at 900 °C in nitrogen for 1 h, distributing the Fe uniformly throughout the sample thickness. The resulting target volume Fe concentration of $3.6 \times 10^{12}\,cm^{-3}$ is well below the solid solubility limit of Fe at 900 °C, (approximately $4 \times 10^{13}\,cm^{-3}$ [8]), hence precipitation is minimized. The low energy and dose used have been shown not to cause any residual damage after annealing that could otherwise affect the carrier lifetime [9].

The samples were then coated with plasma-enhanced chemical-vapour deposited (PECVD) SiN at 400 °C for surface passivation. Effective carrier lifetimes were measured with the quasi-steady-state photoconductance technique (QSSPC) [10]. The interstitial Fe concentration in a 1.2 Ω cm control sample was checked by measurement of the carrier lifetime before and after FeB pair dissociation [11, 12], and was found to be $3.4 \times 10^{12}\,cm^{-3}$, very close to the expected value. Note that the maximum concentration of iron-acceptor pairs in the samples is determined by the implanted iron concentration, which is several orders of magnitude lower than the dopant concentrations.

Knowledge of the dopant concentrations, and especially the net doping $p_0 = N_A - N_D$, is critical to this study. The non-compensated control wafers had resistivities of 0.50, 1.2 and 2.9 Ω cm, corresponding to B concentrations N_A of 3.3×10^{16}, 1.3×10^{16} and $5.3 \times 10^{15}\,cm^{-3}$, respectively.

The compensated samples had resistivities of 0.68 and 2.1 Ω cm, with B concentrations of 7.1×10^{16} and $4.0 \times 10^{16}\,cm^{-3}$, respectively, determined via Fe-acceptor pairing measurements [7]. This method is based on measuring the rate at which the carrier lifetime returns to the initial paired state after optical dissociation of iron-acceptor pairs. The re-pairing rate has been shown to be proportional to the total boron concentration, even in compensated silicon [7]. Previous accurate determination of the proportionality constant [13] allows the measurement of such a rate to be converted into the total boron concentration, as confirmed by comparison with mass spectrometry [4]. The N_A values obtained in this way on the samples studied here with high levels of implanted Fe, are similar to those published previously for other samples from the same ingots with low levels of 'natural' iron [3, 4, 7], providing confidence in the N_A results.

Combining the resistivity and N_A values with Klaassen's mobility model for majority carriers [14, 15], and iterating until the results are self-consistent, leads to estimated P concentrations N_D of 4.2×10^{16} and $3.2 \times 10^{16}\,cm^{-3}$, respectively, and net doping concentrations p_0 of 2.9×10^{16} and $8.5 \times 10^{15}\,cm^{-3}$. It is these p_0 values which determine the recombination activity of impurities such as Fe, in accordance with the Shockley–Read–Hall model [16, 17].

The QSSPC technique requires the sum of the electron and hole mobilities in order to calculate the carrier lifetime from the measured photoconductance. Klaassen's mobility model [14, 15] was used to estimate the mobilities in the compensated samples [4].

3 Results and discussion Figure 1 shows the carrier lifetimes measured by QSSPC within the implanted regions at an excess carrier density of $10^{15}\,cm^{-3}$, as a function of p_0, for both the controls and the compensated samples. The samples were allowed to rest in the dark for 1 day, ensuring that all of the interstitial Fe forms pairs with dopants [18]. Also shown are fits based on the SRH model indicating the expected carrier lifetimes for $3.6 \times 10^{12}\,cm^{-3}$ (calculated from the total implanted dose) of FeB, FeIn or FeGa pairs. Here we have assumed a thermal velocity of 1.1×10^7 cm/s [19] and energy levels and capture cross sections from Refs. [20, 21].

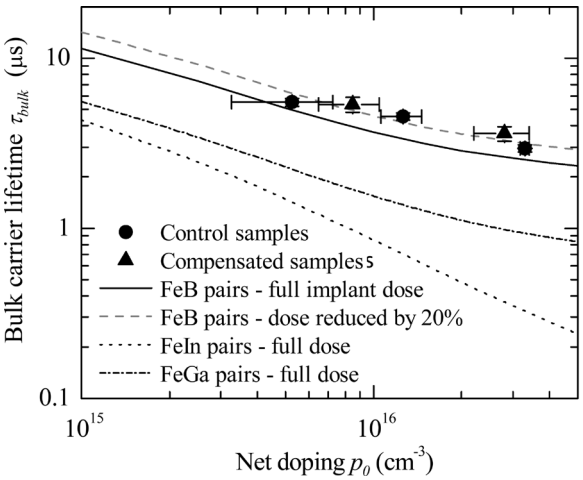

Figure 1 Lifetimes at an excess carrier density of $10^{15}\,cm^{-3}$ as a function of p_0, for the control and compensated samples. Also shown are modelled curves for FeB, FeIn and FeGa pairs for the full implant dose, and an FeB pair concentration reduced by 20%.

The plot shows that the measured lifetimes for both the controls and the compensated samples are near the expected fit for FeB pairs. Indeed, with a reduction in the FeB concentration of just 20%, the agreement is very good, as shown. Such a discrepancy can result from the combined uncertainties in the implanted dose (10%), the carrier lifetime measurements (5% for the controls and 10% for the compensated samples), and the reported values of the capture cross sections (at least 20%). Hence the results are consistent with the Fe being present as FeB pairs in both the control and compensated samples.

Note that the strongly compensated sample with the lowest p_0 value contains $4.0 \times 10^{16}\,cm^{-3}$ of B and $3.2 \times 10^{16}\,cm^{-3}$ of P. If all of the P was present as B–P pairs, as is required to explain the anomalous boron–oxygen defect behaviour, then only $8 \times 10^{15}\,cm^{-3}$ B atoms, or 20% of the total B concentration, would remain isolated. Since it is known [7] that the interstitial Fe can bond equally well with any of the B atoms, irrespective of whether they are paired with P or not, we may infer that only 20% of the Fe-acceptor complexes would be FeB pairs, and the other 80% would be Fe–B–P complexes. Assuming that the recombination properties of Fe–B–P complexes are quite different to those of FeB pairs, we would expect the compensated samples to exhibit significantly different lifetimes to the controls, as exemplified by the large differences shown for FeGa and FeIn pairs. Given that this is not observed, we conclude that the presence of Fe–B–P complexes, and therefore B–P pairs, in the compensated samples is unlikely.

It is of interest to note that the agreement between the compensated and control samples plotted as a function of p_0 confirms that it is indeed the *net doping* that drives the

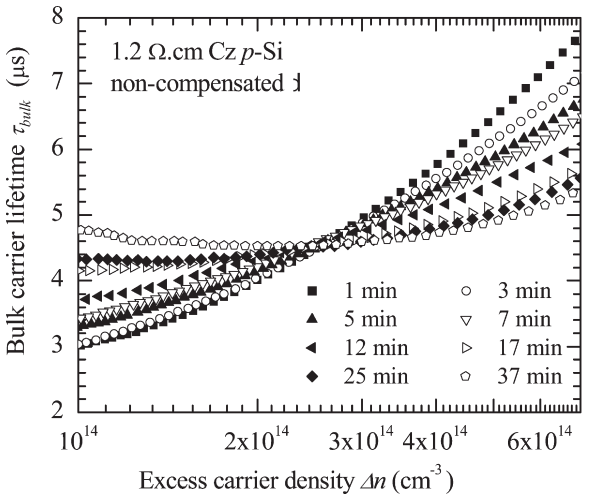

Figure 2 Carrier lifetime *versus* excess carrier density for a non-compensated Fe implanted wafer at various times after dissociation of FeB pairs, showing the crossover point.

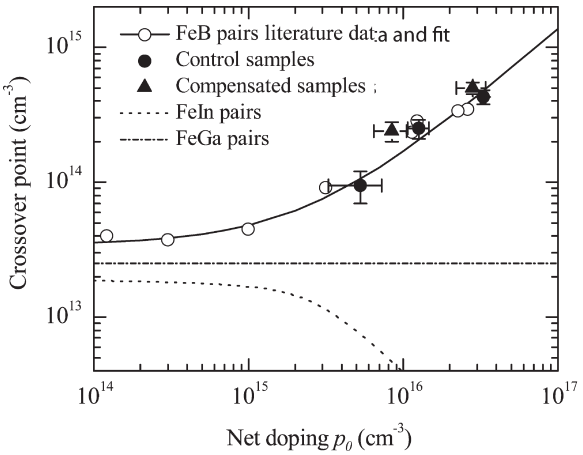

Figure 3 The position of the crossover point *versus* the net doping p_0, for the control and compensated samples. Also shown are previous data for FeB pairs, and modelled curves for FeB, FeIn and FeGa pairs.

recombination activity of the FeB pairs, as expected from the SRH model. This is the basis behind the reduced recombination activity of impurities in compensated Si, as observed recently in solar-grade multicrystalline Si [1].

Additional evidence that the dissolved Fe in the compensated samples is present as FeB pairs can be obtained from the position of the 'crossover' point [20, 22]. The crossover point is defined as the excess carrier density Δn at which the lifetime remains unchanged after dissociation of Fe-acceptor pairs. An example is shown in Fig. 2 after optical dissociation of one of the control samples, revealing the crossover point at $\Delta n = 2.5 \times 10^{14}\,\mathrm{cm}^{-3}$. The position of the crossover point is sensitive to the energy level and capture cross sections of interstitial Fe and the Fe-acceptor pairs present. An advantage of measuring the position of the crossover point, as opposed to the absolute value of the lifetime, is that it is independent of the Fe concentration, making knowledge of the dose unnecessary.

Figure 3 shows measurements of the position of the crossover point in the control and compensated samples, again plotted as a function of the net doping p_0. Also shown are literature data [20] for FeB pairs, and SRH fits based on the known recombination parameters for FeB, FeIn and FeGa pairs. Here we have used parameters for interstitial Fe from Refs. [8, 23]. Again, the measured data for both the controls and the compensated samples align well with the fit for FeB pairs. As outlined above, this implies that the presence of B–P pairs in the compensated samples is only possible if the resulting Fe–B–P complexes have similar recombination properties to FeB pairs.

4 Conclusions Measurement of both the magnitude of the carrier lifetime, and the position of the crossover point upon Fe-acceptor dissociation, reveal that FeB pairs are the dominant Fe-acceptor species in Fe-implanted compensated p-type silicon wafers. This observation is not consistent with the proposed presence of B–P pairs, which should lead to the formation of Fe–B–P complexes, unless these latter complexes happen to have similar recombination properties to FeB pairs.

Acknowledgements D.M. is supported by the Australian Research Council. The authors are grateful to K. Petter and L. J. Geerligs for providing the compensated samples, B. Lim for assisting with surface passivation, and A. Cuevas for helpful discussions.

References

[1] S. Dubois, N. Enjalbert, and J. P. Garandet, Appl. Phys. Lett. **93**, 032114 (2008).
[2] R. Kopecek, J. Arumughan, K. Peter, E. A. Good, J. Libal, M. Acciarri, and S. Binetti, in: Proceedings 23rd European Photovoltaic Solar Energy Conference (WIP-Renewable Energies, Munich, 2008), p. 1855.
[3] B. Lim, A. Liu, D. Macdonald, K. Bothe, and J. Schmidt, Appl. Phys. Lett. **95**, 232109 (2009).
[4] D. Macdonald, F. Rougieux, A. Cuevas, B. Lim, J. Schmidt, M. DiSabatino, and L. J. Geerligs, J. Appl. Phys. **105**, 093704 (2009).
[5] J. Schmidt and K. Bothe, Phys. Rev. B **69**, 024107 (2004).
[6] W. Krühler, C. Moser, F. W. Schulze, and H. Aulich, in: Proceedings 8th European Photovoltaic Solar Energy Conference (Kluwer Academic Publishers, Dordrecht, The Netherlands, 1988), p. 1181.
[7] D. Macdonald, A. Cuevas, and L. J. Geerligs, Appl. Phys. Lett. **92**, 202119 (2008).
[8] A. A. Istratov, H. Hieslmair, and E. R. Weber, Appl. Phys. A **69**, 13 (1999).
[9] D. Macdonald, P. N. K. Deenapanray, and S. Diez, J. Appl. Phys. **96**, 3687 (2004).
[10] R. A. Sinton and A. Cuevas, Appl. Phys. Lett. **69**, 2510 (1996).
[11] G. Zoth and W. Bergholz, J. Appl. Phys. **67**, 6764 (1990).

[12] D. Macdonald, L. J. Geerligs, and A. Azzizi, J. Appl. Phys. **95**, 1021 (2004).
[13] D. Macdonald, T. Roth, P. Deenapanray, K. Bothe, P. Pohl, and J. Schmidt, J. Appl. Phys. **98**, 083509 (2005).
[14] D. B. M. Klaassen, Solid-State Electron. **35**, 953 (1992).
[15] D. B. M. Klaassen, Solid-State Electron. **35**, 961 (1992).
[16] R. N. Hall, Phys. Rev. **87**, 387 (1952).
[17] W. Shockley and W. T. Read, Phys. Rev. **87**, 835 (1952).
[18] L. C. Kimerling and J. L. Benton, Physica **116B**, 297 (1983).
[19] W. M. Bullis and H. R. Huff, J. Electrochem. Soc. **143**, 1399 (1996).
[20] D. Macdonald, T. Roth, P. N. K. Deenapanray, T. Trupke, and R. A. Bardos, Appl. Phys. Lett. **89**, 142107 (2006).
[21] J. Schmidt and D. Macdonald, J. Appl. Phys. **97**, 113712 (2005).
[22] S. Rein and S. W. Glunz, J. Appl. Phys. **98**, 113711 (2005).
[23] D. Macdonald, J. Tan, and T. Trupke, J. Appl. Phys. **103**, 073710 (2008).